Nonlinear Dynamics and Systems Theory, **25** (4) (2025) 386–398

Stability Analysis of a COVID-19 SIR Model with Direct and Indirect Transmission

Akram Boukabache *

Department of Sciences, Teacher Education College of Setif - Messaoud Zeghar, P.O. Box 556, El-Eulma 19600, Sétif, Algeria

Received: July 17, 2024; Revised: July 14, 2025

Abstract: This paper develops a SIR model for COVID-19 that incorporates both direct and indirect transmission dynamics through two distinct incidence rates. To capture the infection rate, we employ a nonlinear Beddington-DeAngelis function and a bilinear incidence function. The model's solutions are shown to be positive and bounded, with two equilibrium points identified: the disease-free equilibrium E_0 and the endemic equilibrium E^*. We establish that E_0 is locally and globally asymptotically stable when the basic reproduction number $R_0 < 1$. Conversely, under specific parameter conditions, E^* is uniformly asymptotically stable for $R_0 > 1$. Numerical simulations are provided to validate the theoretical results.

Keywords: *epidemic model; direct-indirect transmission; incidence function; stability analysis.*

Mathematics Subject Classification (2020): 92B05, 65L10, 93D05, 34D20.

1 Introduction

The COVID-19 pandemic has spurred research across many fields, including the development of mathematical models to assess the impact of interventions on disease control. Kermack and McKendrick [10] pioneered the use of compartmental models for disease dynamics research, leading to the development of various models such as SIR, SIRS, and SEIRS [1, 2, 7, 9, 11, 12].

Incidence functions are crucial in epidemic models as they determine how susceptible individuals transition to infected, significantly influencing model predictions. Epidemiological models often assume well-mixed populations in uniform environments. These models typically use the bilinear incidence rate βSI [10,17] or the standard incidence rate

* Corresponding author: mailto:akramboukabache@gmail.com

$\frac{\beta SI}{N}$ [11,13], where β represents the transmission coefficient and N is the total population. However, when a model incorporates a more realistic population structure with varied mixing patterns and potentially nonlinear transmission dynamics, these standard rates might need adjustments. The probability of infection per contact might be influenced by the number of infected individuals. As the infected population grows, the infection rate may not increase proportionally due to saturation effects, leading to a nonlinear relationship. To address this, nonlinear incidence rates such as the Beddington-DeAngelis rate, $\frac{\beta SI}{1+\alpha_1 S+\alpha_2 I}$, [3, 5] have been incorporated into epidemiological models to better capture the complexities of disease transmission.

Recently, Ahmed et al. [1] conducted a bifurcation analysis of an SIR epidemic model that incorporates both direct and indirect transmission rates. They employed a standard incidence rate, $\frac{\beta SI}{S+I}$, for direct transmission and a bilinear incidence term, βSI, for indirect transmission. This approach takes into account the various ways in which diseases spread through different types of contact. However, their study focused on bifurcation analysis. In this paper, we investigate the stability of an SIR model that incorporates the Beddington-DeAngelis term for direct transmission and the bilinear term for indirect transmission. This combination offers a more realistic representation of transmission dynamics. A constant recruitment rate Λ ensures a steady flow of susceptible individuals due to births. Direct transmission is influenced by the average number of meetings m_i between susceptible and infected individuals within a time interval Δt and the probability of infection success s_c. The Beddington-DeAngelis term $\frac{\beta_d SI}{1+\alpha_1 S+\alpha_2 I}$ captures this, here, $\beta_d = m_i s_c > 0$ and $\frac{S}{1+\alpha_1 S+\alpha_2 I}$ is the proportion of the susceptible population in time t. In contrast, indirect transmission occurs when susceptible individuals come into contact with the virus on surfaces, without directly interacting with infected individuals. This is modeled as a mass contact process with an indirect infection rate $\beta_i > 0$. The bilinear incidence term $\beta_i SI$ represents the rate of indirect COVID-19 transmission through contaminated surfaces. To the best of our knowledge, there is no SIR model that combines direct (Beddington-DeAngelis) and indirect (bilinear) transmissions.

The manuscript is organized as follows. Section 2 establishes the well-posedness of the model by demonstrating the existence, positivity, and boundedness of its solutions. In Section 3, we analyze the model, compute the basic reproduction number, and prove the existence of equilibria. Section 4 delves into the analytical properties of the model, including the stability analysis of the equilibria. Numerical simulations are given in Section 5, and concluding remarks are offered in the closing section.

2 Model Formulation and Analysis

We consider the total population at time t, it is denoted by $N(t)$ and divided into three compartments: susceptible individuals $S(t)$, infected individuals $I(t)$ and recovered individuals $R(t)$, where $N(t) = S(t)+I(t)+R(t)$. Susceptible individuals are healthy but vulnerable to infection, while infected individuals can transmit the disease and eventually transit to the recovered state, either through immunity or treatment.

Based on the previous assumptions, the SIR model with direct and indirect transmis-

sions is described by the following system of differential equations:

$$\begin{aligned}
\frac{dS}{dt} &= \Lambda - \frac{\beta_d SI}{1+\alpha_1 S+\alpha_2 I} - \beta_i SI - \mu S,\\
\frac{dI}{dt} &= \frac{\beta_d SI}{1+\alpha_1 S+\alpha_2 I} + \beta_i SI - (d+\gamma+\mu)\, I,\\
\frac{dR}{dt} &= \gamma I - \mu R
\end{aligned} \tag{1}$$

with the given initial conditions $S(0) \geq 0, I(0) \geq 0$ and $R(0) \geq 0$.

The parameters involved in this model and their corresponding interpretations are given in Table 2. The flowchart of the SIR model is illustrated in Figure 1.

Parameter	Description
Λ	Recruitment rate
β_d	Direct transmission rate
β_i	Indirect transmission rate
α_1	Measure of inhibition (taken by susceptibles)
α_2	Measure of inhibition (taken by infectives)
μ	Natural death rate
d	Infection death rate
γ	Natural recovery rate

Table 1: Description of biological parameters.

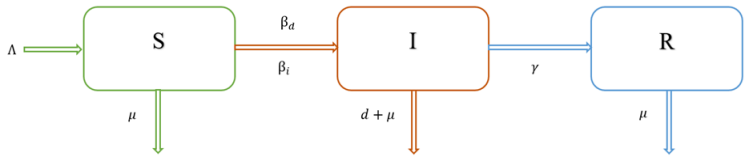

Figure 1: Flowchart of the proposed model.

For problems concerning population dynamics, it is crucial to ensure that solutions remain non-negative and bounded for all time. To achieve this, we define the region $\Omega = \{(S,I,R) \in \mathbb{R}^3_+ : S \geq 0, I \geq 0, R \geq 0\}$.

Theorem 2.1 *For any non-negative initial data, the solutions of* (1) *exist, remain bounded and non-negative in* Ω. *Moreover, we have*

$$N(t) \leq \frac{\Lambda}{\mu}.$$

Proof. Based on the well-established theory of differential equations in a functional framework (see, e.g., [8]), we can ensure a unique local solution for problem (1). To establish solution positivity, we prove invariance of the positive set Ω. We have

$$\left.\frac{dS}{dt}\right|_{S=0} = \Lambda > 0, \qquad \left.\frac{dI}{dt}\right|_{I=0} = 0 \geq 0, \qquad \left.\frac{dR}{dt}\right|_{R=0} = \gamma I \geq 0.$$

Hence, for all $t \geq 0$, the positivity of all solutions initiating in Ω is guaranteed.

For the boundedness, we utilize the fact that $N = S + I + R$. By summing the equations of the model (1), we have

$$\frac{dN}{dt} = \Lambda - \mu N - dI.$$

As $I \geq 0$, we get

$$\frac{dN}{dt} \leq \Lambda - \mu N,$$

and therefore,

$$N(t) \leq \frac{\Lambda}{\mu} + \left(N(0) - \frac{\Lambda}{\mu}\right) e^{-\mu t}.$$

Thus, $\lim_{t\to\infty} \sup N(t) \leq \frac{\Lambda}{\mu}$ and $\frac{dN}{dt} < 0$ if $N > \frac{\Lambda}{\mu}$. This reveals that the total population size $N(t)$ is bounded, and so is each compartment $S(t)$, $I(t)$ and $R(t)$.

3 The Steady States

The existence of a disease-free equilibrium (DFE) and that of an endemic equilibrium for our model are established in this subsection. Due to the fact that the first two equations of the system (1) are not affected by $R(t)$, and considering that the total population number is $N(t) = S(t) + I(t) + R(t)$, we may omit the last equation of the system (1). As a result, the problem can be reduced to

$$\begin{aligned} \frac{dS}{dt} &= \Lambda - \frac{\beta_d SI}{1 + \alpha_1 S + \alpha_2 I} - \beta_i SI - \mu S, \\ \frac{dI}{dt} &= \frac{\beta_d SI}{1 + \alpha_1 S + \alpha_2 I} + \beta_i SI - \delta I, \end{aligned} \tag{2}$$

where $\delta = d + \gamma + \mu$ and $S, I \geq 0$.

In order to find the equilibria of the system (2), we solve the following system:

$$\Lambda - \frac{\beta_d SI}{1 + \alpha_1 S + \alpha_2 I} - \beta_i SI - \mu S = 0,$$

$$\frac{\beta_d SI}{1 + \alpha_1 S + \alpha_2 I} + \beta_i SI - \delta I = 0.$$

Obviously, $E_0 = \left(\frac{\Lambda}{\mu}, 0\right)$ is the DFE of (2).

When the system reaches the DFE point E_0, the disease vanishes completely. At this point, the infected population becomes zero, and the remaining population consists only of susceptible individuals.

3.1 Basic reproduction number

The basic reproduction number R_0 is crucial in epidemiology as it predicts disease spread and informs control strategies. It estimates the average number of new infections caused by one infected individual. By using the next-generation matrix method [15], we can easily find R_0. Let $X(t) = (S(t), I(t))$, then it follows from model (2) that

$$\frac{dX}{dt} = \mathcal{F} - \mathcal{V},$$

where

$$\mathcal{F} = \begin{pmatrix} \Lambda - \frac{\beta_d SI}{1+\alpha_1 S+\alpha_2 I} - \beta_i SI \\ \frac{\beta_d SI}{1+\alpha_1 S+\alpha_2 I} + \beta_i SI \end{pmatrix} \qquad \text{and} \qquad \mathcal{V} = \begin{pmatrix} \mu S \\ \delta I \end{pmatrix}.$$

So, the Jacobian matrices of new infected terms $\mathcal{F}$ and other transfer terms $\mathcal{V}$ at E_0 are

$$F = \begin{pmatrix} 0 & -\frac{\beta_d \Lambda}{\mu+\alpha_1 \Lambda} - \frac{\beta_i \Lambda}{\mu} \\ 0 & \frac{\beta_d \Lambda}{\mu+\alpha_1 \Lambda} + \frac{\beta_i \Lambda}{\mu} \end{pmatrix} \qquad \text{and} \qquad V = \begin{pmatrix} \mu & 0 \\ 0 & \delta \end{pmatrix}.$$

So

$$FV^{-1} = \begin{pmatrix} 0 & -\frac{\beta_d \Lambda}{(\mu+\alpha_1 \Lambda)\delta} - \frac{\beta_i \Lambda}{\mu\delta} \\ 0 & \frac{\beta_d \Lambda}{(\mu+\alpha_1 \Lambda)\delta} + \frac{\beta_i \Lambda}{\mu\delta} \end{pmatrix}.$$

As R_0 is the spectral radius of FV^{-1}, we get

$$R_0 = \frac{\beta_d \Lambda}{(\mu + \alpha_1 \Lambda)\,\delta} + \frac{\beta_i \Lambda}{\mu\delta} = R_0^d + R_0^i.$$

Note that R_0^d represents the basic reproduction number for only direct transmission, where a susceptible individual becomes infected through contact with an infected individual R_0^i, on the other hand, it captures the contribution of indirect transmission, where an infected individual contaminates the environment, leading to subsequent infections. Public health interventions can target these specific pathways. Quarantine measures reduce direct transmission, lowering R_0^d. Improved hygiene practices reduce indirect transmission, lowering R_0^i. Consequently, the overall ability of the disease to spread (reflected by R_0) will also go down. This makes sense because there are fewer ways for people to catch it.

3.2 Existence of endemic equilibrium

In the presence of infection, we show, in the following result, that the system (2) has a unique endemic equilibrium.

Theorem 3.1 *If $R_0 > 1$, the model (2) has a unique endemic equilibrium point $E^* = (S^*, I^*)$.*

Proof. Consider the system (2), where $E^* = (S^*, I^*)$,

$$\begin{aligned} \frac{\beta_d S^* I^*}{1 + \alpha_1 S^* + \alpha_2 I^*} + \beta_i S^* I^* &= \Lambda - \mu S^*, \\ \frac{\beta_d S^* I^*}{1 + \alpha_1 S^* + \alpha_2 I^*} + \beta_i S^* I^* &= \delta I^*, \end{aligned} \tag{3}$$

which implies that

$$\Lambda - \mu S^* = \delta I^*.$$

We get S^* as a function of I^* as follows:

$$S^* = \frac{\Lambda - \delta I^*}{\mu}. \tag{4}$$

Now, we take the S^* quadratic equation out from the first equation of (3) as

$$\alpha_1 (\beta_i I^* + \mu) S^{*^2} + (\beta_d I^* - \alpha_1 \Lambda + (\beta_i I^* + \mu)(1 + \alpha_2 I^*)) S^* - \Lambda (1 + \alpha_2 I^*) = 0. \quad (5)$$

Substituting (4) into (5) gives the cubic equation in I^*:

$$a_1 (I^*)^3 + a_2 (I^*)^2 + a_3 I^* = 0,$$

where

$$\begin{aligned} a_1 &= \delta\beta_i (\delta\alpha_1 - \mu\alpha_2), \\ a_2 &= \delta\mu (\delta\alpha_1 - \mu\alpha_2) + \beta_i\Lambda (2\delta\alpha_1 - \mu\alpha_2) - \delta\mu (\beta_i + \beta_d), \\ a_3 &= \mu\Lambda\beta_d + \Lambda\beta_i (\mu + \Lambda\alpha_1) - \delta\mu (\mu + \alpha_1\Lambda). \end{aligned}$$

The constant term a_3 can be rewritten as

$$\begin{aligned} a_3 &= \delta\mu (\mu + \alpha_1\Lambda) \left(\frac{\Lambda\beta_d}{\delta (\mu + \alpha_1\Lambda)} + \frac{\Lambda\beta_i}{\delta\mu} - 1 \right) \\ &= \delta\mu (\mu + \alpha_1\Lambda)(R_0 - 1). \end{aligned}$$

It is easily seen that $a_3 > 0$ if $R_0 > 1$. Additionally, we note that $a_1, a_2 < 0$ if $2\delta\alpha_1 < \mu\alpha_2$. According to the Descartes rule of signs, see Wang [16], the equation (2) possesses a unique non-negative I^*.

The value of S^* is then calculated using equation (4). As a result, the model (2) has a unique endemic equilibrium point $E^* = (S^*, I^*)$ if $R_0 > 1$.

4 Stability Analysis

4.1 Local stability

The local stability results for the model (2) are ensured by the following results.

Theorem 4.1 *If $R_0 < 1$, the model (2) at E_0 is locally asymptotically stable and unstable for $R_0 > 1$.*

Proof. The Jacobian matrix of the system (2) at E_0 is given by

$$J = \begin{pmatrix} -\mu & -\frac{\beta_d\Lambda}{\mu+\alpha_1\Lambda} - \frac{\beta_i\Lambda}{\mu} \\ 0 & \frac{\beta_d\Lambda}{\mu+\alpha_1\Lambda} + \frac{\beta_i\Lambda}{\mu} - \delta \end{pmatrix}.$$

The eigenvalues of J are $\lambda_1 = -\mu$ and $\lambda_2 = \delta (R_0 - 1)$. The matrix J has negative eigenvalues when $R_0 < 1$. Thus, E_0 of the model (2) is locally asymptotically stable. If $R_0 > 1$, the eigenvalue $\lambda_2 > 0$, so E_0 is unstable.

Theorem 4.2 *If $R_0 > 1$, the model (2) at the disease endemic equilibrium point E^* is locally asymptotically stable under the following conditions:*

$$\frac{\beta_d S^* (1 + \alpha_1 S^*)}{(1 + \alpha_1 S^* + \alpha_2 I^*)^2} < l, \quad (6)$$

where

$$l = \min \left(\mu + \delta + \frac{\beta_d I^* (1 + \alpha_2 I^*)}{(1 + \alpha_1 S^* + \alpha_2 I^*)^2} + \beta_i I^*, \delta + \frac{\beta_d I^* (1 + \alpha_2 I^*)\delta}{\mu (1 + \alpha_1 S^* + \alpha_2 I^*)^2} + \frac{\beta_i I^* \delta}{\mu} \right).$$

Proof. The Jacobian matrix of the system (2) at E^* is given by

$$J(E^*) = \begin{pmatrix} -\mu - \frac{\beta_d I^*(1+\alpha_2 I^*)}{(1+\alpha_1 S^*+\alpha_2 I^*)^2} - \beta_i I^* & -\frac{\beta_d S^*(1+\alpha_1 S^*)}{(1+\alpha_1 S^*+\alpha_2 I^*)^2} - \beta_i S^* \\ \frac{\beta_d I^*(1+\alpha_2 I^*)}{(1+\alpha_1 S^*+\alpha_2 I^*)^2} + \beta_i I^* & \frac{\beta_d S^*(1+\alpha_1 S^*)}{(1+\alpha_1 S^*+\alpha_2 I^*)^2} + \beta_i S^* - \delta \end{pmatrix}.$$

The characteristics equation $\det(J - \lambda I)$ associated to $J(E^*)$ is derived and given as

$$\lambda^2 + a_1\lambda + a_2 = 0, \tag{7}$$

where

$$a_1 = \mu + \delta + \frac{\beta_d I^*(1+\alpha_2 I^*)}{(1+\alpha_1 S^*+\alpha_2 I^*)^2} + \beta_i I^* - \frac{\beta_d S^*(1+\alpha_1 S^*)}{(1+\alpha_1 S^*+\alpha_2 I^*)^2} - \beta_i S^*,$$

$$a_2 = \mu\delta + \frac{\beta_d I^*(1+\alpha_2 I^*)\delta}{(1+\alpha_1 S^*+\alpha_2 I^*)^2} + \beta_i I^*\delta - \frac{\mu\beta_d S^*(1+\alpha_1 S^*)}{(1+\alpha_1 S^*+\alpha_2 I^*)^2} - \mu\beta_i S^*.$$

Thanks to the assumption (6), we know that $a_i > 0, i = 1, 2$. Therefore, by the Routh–Hurwitz criterion [4], all roots of (7) have negative real parts. Thus, E^* is locally asymptotically stable.

Remark 4.1 Taking into account the sign of real parts of λ in (7), we can establish the following:

- if
$$\mu\delta + \frac{\beta_d I^*(1+\alpha_2 I^*)\delta}{(1+\alpha_1 S^*+\alpha_2 I^*)^2} + \beta_i I^*\delta < \frac{\mu\beta_d S^*(1+\alpha_1 S^*)}{(1+\alpha_1 S^*+\alpha_2 I^*)^2} + \mu\beta_i S^*, \tag{8}$$
the endemic equilibrium E^* is a saddle point.
- if
$$\mu + \delta + \frac{\beta_d I^*(1+\alpha_2 I^*)}{(1+\alpha_1 S^*+\alpha_2 I^*)^2} + \beta_i I^* < \frac{\beta_d S^*(1+\alpha_1 S^*)}{(1+\alpha_1 S^*+\alpha_2 I^*)^2} + \beta_i S^*, \tag{9}$$
the endemic equilibrium E^* is unstable.

4.2 Global stability

We employed a Lyapunov function to analyze the global stability of both the DFE and endemic equilibrium of the system. The stability of the DFE is established by the following theorem.

Theorem 4.3 *If $R_0 \leq 1$, the model (2) at the DFE E_0 is globally asymptotically stable.*

Proof. We consider the following Lyapunov function:

$$L(S, I) = \frac{1}{1+\alpha_1 S^0}\left(S - S^0 - S^0 \ln\frac{S}{S^0}\right) + I. \tag{10}$$

Taking derivative of (10) with respect to time t, one has

$$\begin{aligned}\frac{dL}{dt}(S, I) &= \frac{1}{1+\alpha_1 S^0}\left(1 - \frac{S^0}{S}\right)\frac{dS}{dt} + \frac{dI}{dt} \\ &= \frac{1}{1+\alpha_1 S^0}\left(1 - \frac{S^0}{S}\right)\left(\Lambda - \frac{\beta_d SI}{1+\alpha_1 S+\alpha_2 I} - \beta_i SI - \mu S\right) \\ &\quad + \frac{\beta_d SI}{1+\alpha_1 S+\alpha_2 I} + \beta_i SI - \delta I.\end{aligned}$$

Given that $S^0 = \frac{\Lambda}{\mu}$ and after simplification, we have

$$\begin{aligned}
\frac{dL}{dt} &= \frac{-\mu\left(S^0 - S\right)^2}{\left(1+\alpha_1 S^0\right)S} + \frac{\delta I}{\left(1+\alpha_1 S+\alpha_2 I\right)}R_0^d + \frac{\delta\alpha_1 SI}{\left(1+\alpha_1 S+\alpha_2 I\right)}R_0^d \\
&\quad - \delta I + \frac{\delta I\left(1+\alpha_1 S\right)}{\left(1+\alpha_1 S^0\right)}R_0^i \\
&= \frac{-\mu\left(S^0 - S\right)^2}{\left(1+\alpha_1 S^0\right)S} + \frac{\delta I}{\left(1+\alpha_1 S+\alpha_2 I\right)}\left(R_0^d - 1\right) \\
&\quad + \frac{\delta\alpha_1 SI}{\left(1+\alpha_1 S+\alpha_2 I\right)}\left(R_0^d - 1\right) - \frac{\delta\alpha_2 I^2}{1+\alpha_1 S+\alpha_2 I} + \frac{\delta I\left(1+\alpha_1 S\right)}{\left(1+\alpha_1 S^0\right)}R_0^i \\
&= \frac{-\mu\left(S^0 - S\right)^2}{\left(1+\alpha_1 S^0\right)S} + \frac{P}{1+\alpha_1 S+\alpha_2 I}\left(R_0^d - 1\right) - \frac{\delta\alpha_2 I^2}{1+\alpha_1 S+\alpha_2 I} \\
&\quad + \frac{P}{\left(1+\alpha_1 S^0\right)}R_0^i,
\end{aligned}$$

where $P = \delta\left(\alpha_1 S + 1\right)I$. We end the proof by noting that

$$\begin{aligned}
&\frac{P}{1+\alpha_1 S+\alpha_2 I}\left(R_0^d - 1\right) + \frac{P}{\left(1+\alpha_1 S^0\right)}R_0^i \\
&\leq \frac{P}{\left(1+\alpha_1 S+\alpha_2 I\right)}\left(R_0 - 1\right) + \frac{P}{\left(1+\alpha_1 S^0\right)}\left(R_0 - 1\right).
\end{aligned}$$

Thus

$$\begin{aligned}
\frac{dL}{dt} &\leq \frac{-\mu\left(S^0 - S\right)^2}{\left(1+\alpha_1 S^0\right)S} + \frac{P\left(\left(1+\alpha_1 S^0\right) + \left(1+\alpha_1 S+\alpha_2 I\right)\right)}{\left(1+\alpha_1 S+\alpha_2 I\right)\left(1+\alpha_1 S^0\right)}\left(R_0 - 1\right) \\
&\quad - \frac{\delta\alpha_2 I^2}{1+\alpha_1 S+\alpha_2 I}.
\end{aligned}$$

It is obvious that $\frac{dL}{dt} < 0$ if $R_0 \leq 1$ for all $(S, I) \neq \left(S^0, 0\right)$. Also, $\frac{dL}{dt} = 0$ if and only if (S, I) is at E_0. Hence, the La Salle invariance principle states that the DFE point of system (2) is globally asymptotically stable.

Theorem 4.4 *If $R_0 > 1$, the model (2) at the endemic equilibrium E^* is globally asymptotically stable under the following conditions:*

$$\left(\frac{1+\alpha_1 S^* + \alpha_2 I^*}{1+\alpha_1 S+\alpha_2 I} - 1\right)\left(\frac{I^*}{I} - \frac{S^*}{S}\right) \leq 0. \tag{11}$$

Proof. We consider the following Lyapunov function:

$$L\left(t\right) = S - S^* - S^* \ln\frac{S}{S^*} + \left(I - I^* - I^* \ln\frac{I}{I^*}\right). \tag{12}$$

Taking the time derivative of (12), we have

$$\frac{dL\left(t\right)}{dt} = \left(1 - \frac{S^*}{S}\right)\frac{dS\left(t\right)}{dt} + \left(1 - \frac{I^*}{I}\right)\frac{dI\left(t\right)}{dt}.$$

Substituting the values of $\frac{dS(t)}{dt}$ and $\frac{dI(t)}{dt}$ into the above equation, and using the equalities

$$\Lambda = \frac{\beta_d S^* I^*}{1+\alpha_1 S^* + \alpha_2 I^*} + \beta_i S^* I^* + \mu S^*,$$
$$\delta I^* = \frac{\beta_d S^* I^*}{1+\alpha_1 S^* + \alpha_2 I^*} + \beta_i S^* I^*$$

give

$$\begin{aligned}
\frac{dL(t)}{dt} &= \left(1-\frac{S^*}{S}\right) \\
&\left(\frac{\beta_d S^* I^*}{1+\alpha_1 S^* + \alpha_2 I^*} + \beta_i S^* I^* + \mu S^* - \frac{\beta_d SI}{1+\alpha_1 S + \alpha_2 I} - \beta_i SI - \mu S\right) \\
&+ \left(1-\frac{I^*}{I}\right)\left(\frac{\beta_d SI}{1+\alpha_1 S+\alpha_2 I} + \beta_i SI - \delta I\right) \\
&= -\mu\frac{(S-S^*)^2}{S} + \frac{\beta_d S^* I^*}{1+\alpha_1 S^* + \alpha_2 I^*} + \beta_i S^* I^* - \frac{\beta_d SI}{1+\alpha_1 S+\alpha_2 I} \\
&- \beta_i SI - \frac{\beta_d (S^*)^2 I^*}{S(1+\alpha_1 S^* + \alpha_2 I^*)} - \frac{\beta_i (S^*)^2 I^*}{S} + \frac{\beta_d S^* I}{1+\alpha_1 S+\alpha_2 I} \\
&+ \beta_i S^* I + \frac{\beta_d SI}{1+\alpha_1 S+\alpha_2 I} + \beta_i SI - \frac{\beta_d S^* I}{1+\alpha_1 S^* + \alpha_2 I^*} \\
&- \beta_i S^* I - \frac{\beta_d SI^*}{1+\alpha_1 S+\alpha_2 I} - \beta_i SI^* + \frac{\beta_d S^* I^*}{1+\alpha_1 S^* + \alpha_2 I^*} + \beta_i S^* I^*.
\end{aligned}$$

It follows that

$$\begin{aligned}
\frac{dL(t)}{dt} &= \mu\left(2-\frac{S^*}{S}-\frac{S}{S^*}\right) + \beta_i S^* I^*\left(2-\frac{S^*}{S}-\frac{S}{S^*}\right) \\
&+ \frac{\beta_d S^* I^*}{1+\alpha_1 S^* + \alpha_2 I^*}\left(2-\frac{S^*}{S}-\frac{S}{S^*}\right) + \frac{\beta_d S^* I^*}{1+\alpha_1 S^* + \alpha_2 I^*} \\
&\left(\frac{I(1+\alpha_1 S^* + \alpha_2 I^*)}{I^*(1+\alpha_1 S+\alpha_2 I)} - \frac{I}{I^*} - \frac{S(1+\alpha_1 S^* + \alpha_2 I^*)}{S^*(1+\alpha_1 S+\alpha_2 I)} + \frac{S}{S^*}\right) \\
&= \left(\mu + \frac{\beta_d S^* I^*}{1+\alpha_1 S^* + \alpha_2 I^*} + \beta_i S^* I^*\right)\left(1-\frac{S^*}{S}\right)\left(1-\frac{S}{S^*}\right) \\
&+ \frac{\beta_d S^* I^*}{1+\alpha_1 S^* + \alpha_2 I^*}\left(\frac{1+\alpha_1 S^* + \alpha_2 I^*}{1+\alpha_1 S+\alpha_2 I} - 1\right)\left(\frac{I^*}{I} - \frac{S^*}{S}\right).
\end{aligned}$$

Clearly,

$$\left(1-\frac{S^*}{S}\right)\left(1-\frac{S}{S^*}\right) \le 0,$$

and by (11),

$$\left(\frac{1+\alpha_1 S^* + \alpha_2 I^*}{1+\alpha_1 S+\alpha_2 I} - 1\right)\left(\frac{I^*}{I} - \frac{S^*}{S}\right) \le 0,$$

where strict equality holds when $S = S^*$ and $I = I^*$. Thus, E^* is globally asymptotically stable.

5 Numerical Simulations

In this section, we assess the computational performance of the SIR model (2). We employed the Non-standard Finite Difference scheme for the numerical simulations. All numerical simulations and figure generations were performed in Matlab

5.1 Stability of disease-free equilibrium

In a disease-free equilibrium, the infection is completely absent among the population. The specific values used for the biological parameters are presented in Table 2 [14].

Parameter	Value
Λ	5
β_d	0.003
β_i	0.00006 (Assumed)
α_1	0.002
α_2	0.001
μ	0.05
d	0.06
γ	0.002

Table 2: Parameter values.

For these values of parameters, $R_0 < 1$ and E_0 exists at $(250, 0)$. This implies that the disease eventually disappear from the population. As shown in Figure 2, the solutions of the system (2) with the initial values $S(0) = 85$ and $I(0) = 12$ converge towards E_0, which confirms that that E_0 is globally asymptotically stable.

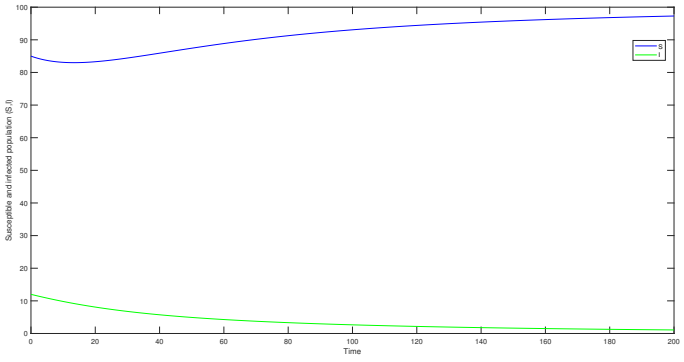

Figure 2: Dynamical behavior of the susceptible and infected populations.

5.2 Stability of endemic equilibrium

We choose the set of parameters given in Table 3 [6].

We find that $R_0 > 1$ and the condition $2\delta\alpha_1 < \mu\alpha_2$ holds. The numerical solutions, depicted in Figure 3, show that the susceptible and infected populations, with the initial

Parameter	Value
Λ	7
β_d	0.003
β_i	0.0000001 (Assumed)
α_1	0.002
α_2	0.5
μ	0.02
d	0.05
γ	0.002

Table 3: Parameter values.

values $S(0) = 250$ and $I(0) = 45$, converge towards an endemic equilibrium point $E^* = (277.8749, 20.0348)$. This indicates that E^* is globally asymptotically stable.

Furthermore, in Figure 4, we utilize the parameters from Table 4 to demonstrate that $E^* = (5.2041, 3.5738)$ is globally asymptotically stable. This implies that, for the given parameter set, the trajectories of both S and I will converge towards the same steady-state value of E^* regardless of the initial values assigned to S and I.

Parameter	Value
Λ	1.97
β_d	0.05
β_i	0.01 (Assumed)
α_1	0.001
α_2	0.1
μ	0.2
d	0.03
γ	0.03

Table 4: Parameter values.

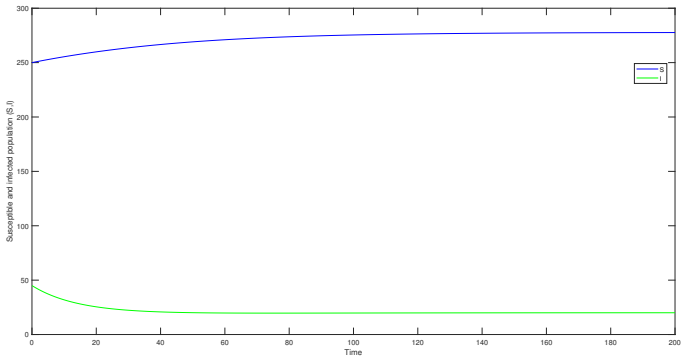

Figure 3: Dynamical behavior of the susceptible and infected populations.

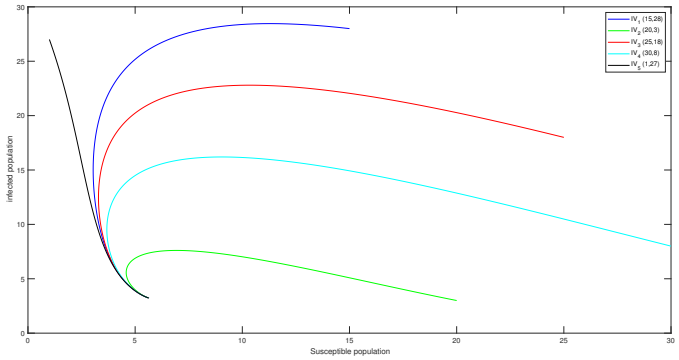

Figure 4: Global stability of the endemic equilibrium point.

6 Conclusion

This study developed a SIR model incorporating both direct and indirect transmission pathways to investigate the dynamics of COVID-19. By utilizing a Beddington-DeAngelis infection rate and a bilinear incidence term, the model captured the intricate complexities of disease spread. The model's well-posedness was confirmed through the identification of a positively invariant region. A rigorous analysis of the DFE E_0 and endemic equilibrium E^* is conducted. The basic reproduction number R_0 is decomposed into its direct R_0^d and indirect R_0^i components, reflecting the dual transmission mechanisms. Our findings demonstrate that E_0 is both locally and globally asymptotically stable when $R_0 < 1$, indicating disease eradication. Conversely, for $R_0 > 1$, E_0 becomes unstable, giving rise to E^*. The local and global stability of E^* is investigated under specific conditions.

The findings underscore that to effectively eradicate the disease ($R_0 < 1$), a comprehensive approach is needed targeting both R_0^d and R_0^i. Reducing R_0^d through measures such as mask-wearing, social distancing, and improved ventilation, in conjunction with decreasing R_0^i via hand hygiene and surface disinfection, is crucial. By quantifying the relative contributions of these transmission modes to the overall R_0, policymakers can optimize resource allocation and implement targeted control strategies. For instance, environments with high levels of indirect transmission (e.g., hospitals, nursing homes) necessitate enhanced cleaning protocols and personal protective equipment to reduce disease spread.

This study provides a basic framework for understanding COVID-19 transmission dynamics. Future investigations should incorporate additional factors such as age structure and vaccination to refine the model's predictive accuracy. By combining these insights with real-world data, we can develop more effective public health measures to protect communities from subsequent outbreaks.

References

[1] M. Ahmed, M.H.O.R. Khan and M.M. Alam Sarker. COVID-19 SIR model: Bifurcation analysis and optimal control. *Results in Control and Optimization* **12** (2023) 100246.

[2] A.Y.P. Asih, B. Gunawan, N. Hidayati, T. Herlambang, D. Rahmalia and K. Oktafianto. Weights optimization using firefly algorithm for dengue fever optimal control model by

vaccination, treatment and abateseae. *Nonlinear Dynamics and Systems Theory* **23** (3) (2023) 237–248.

[3] J.R. Beddington. Mutual interference between parasites or predators and its effect on searching efficiency. *The Journal of Animal Ecology* (1975) 331–340.

[4] N.P. Bhatia and G.P. Szegő. *Stability Theory of Dynamical Systems*. Springer-Verlag, Berlin, 1970.

[5] D.L. DeAngelis, R.A. Goldstein, and R.V. O'Neill. A model for tropic interaction. *Ecology* **56** (4) (1975) 881–892.

[6] B. Dubey, P. Dubey, and U.S. Dubey. Dynamics of an SIR model with nonlinear incidence and treatment rate. *Applications and Applied Mathematics: An International Journal (AAM)* **10** (2) (2015) 5.

[7] M. El Hassnaoui, S. Melliani, and M. Oukessou. Application of accretive operators theory to linear SIR model. *Nonlinear Dynamics and Systems Theory* (2022) 379.

[8] J.K. Hale and S.M.V. Lunel. *Introduction to Functional Differential Equations*. Springer Science & Business Media, Berlin, 2013.

[9] Y. Jin, W. Wang, and S. Xiao. An SIRS model with a nonlinear incidence rate. *Chaos, Solitons & Fractals* **34** (5) (2007) 1482–1497.

[10] W.O. Kermack and A.G. McKendrick. A contribution to the mathematical theory of epidemics. *Proceedings of the Royal Society of London. Series A, Containing papers of a mathematical and physical character* **115** (772) (1927) 700–721.

[11] A. Korobeinikov and G.C. Wake. Lyapunov functions and global stability for SIR, SIRS, and SIS epidemiological models. *Applied Mathematics Letters* **15** (8) (2002) 955–960.

[12] H. Ouedraogo and A. Guiro. Analysis of dengue disease transmission model with general incidence functions. *Nonlinear Dynamics and Systems Theory* (2023).

[13] M. Parsamanesh and M. Erfanian. Global dynamics of an epidemic model with standard incidence rate and vaccination strategy. *Chaos, Solitons & Fractals* **117** (2018) 192–199.

[14] Swati and Nilam. Fractional order SIR epidemic model with Beddington–De Angelis incidence and Holling type II treatment rate for COVID-19. *Journal of Applied Mathematics and Computing* **68** (6) (2022) 3835–3859.

[15] P. van den Driessche and J. Watmough. Reproduction numbers and sub-threshold endemic equilibria for compartmental models of disease transmission. *Mathematical Biosciences* **180** (1–2) (2002) 29–48.

[16] X. Wang. A simple proof of Descartes's rule of signs. *The American Mathematical Monthly* **111** (6) (2004) 525–526.

[17] F. Zhang, Z.-z. Li and F. Zhang. Global stability of an SIR epidemic model with constant infectious period. *Applied Mathematics and Computation* **199** (1) (2008) 285–291.